Low Temperature Physics/Fizika Nizkikh Temperatur, 2016, v. 42, No. 7, pp. 764–769

Positron annihilation characterization of free volume in micro- and macro-modified $Cu_{0.4}Co_{0.4}Ni_{0.4}Mn_{1.8}O_4$ ceramics

H. Klym[1], A. Ingram[2], O. Shpotyuk[3,4], I. Hadzaman[5], V. Solntsev[6], O. Hotra[7], and A.I. Popov[8]

[1]*Lviv Polytechnic National University, Ukraine*
E-mail: klymha@yahoo.com; halyna.i.klym@lpnu.ua

[2]*Physics Faculty of Opole University of Technology, Poland*

[3]*Vlokh Institute of Physical Optics, Lviv, Ukraine*

[4]*Institute of Physics of Jan Dlugosz University, Poland*

[5]*Drohobych Ivan Franko State Pedagogical University, Ukraine*

[6]*V.E. Lashkaryov Institute of Semiconductor Physics of the National Academy of Sciences of Ukraine, Kiev, Ukraine*

[7]*Lublin University of Technology, Poland*

[8]*Institute of Solid State Physics, University of Latvia, Latvia*

Received May 4, 2016, published online May 25, 2016

Free volume and pore size distribution size in functional micro and macro-micro-modified $Cu_{0.4}Co_{0.4}Ni_{0.4}Mn_{1.8}O_4$ ceramics are characterized by positron annihilation lifetime spectroscopy in comparison with Hg-porosimetry and scanning electron microscopy technique. Positron annihilation results are interpreted in terms of model implication positron trapping and ortho-positronium decaying. It is shown that free volume of positron traps are the same type for macro and micro modified $Cu_{0.4}Co_{0.4}Ni_{0.4}Mn_{1.8}O_4$ ceramics. Classic Tao-Eldrup model in spherical approximation is used to calculation of the size of nanopores smaller than 2 nm using the ortho-positronium lifetime.

PACS: 78.70.Bj Positron annihilation;
71.60.+z Positron states;
81.05.Mh Cermets, ceramic and refractory composites;
82.30.Gg Positronium chemistry.

Keywords: ceramics, free volume, nanopores, positron trapping, positronium decaying.

1. Introduction

Functional fine-grained temperature-sensitive ceramics based on transition-metal manganites is one of the typical representatives of so-called topologically disordered substances having wide industrial applications [1–3]. Adequate understanding of correlation between porous and void structures of such materials is still in focus of scientific and commercial interests [4,5]. The spatial ordering arrangement in atomic positions is taken as main determinant for their functional properties. In bulk ceramics, depending on the sintering condition (mainly temperature), a significant shrinkage of the atomic structure occurs, eventually leading to more or less complex pore topology [6–8]. These pores along with specific vacancy-type defects within crystalline grains and grain boundaries represent free-volume (void) structure of ceramics. Thus, not only grain but also pores determine main characteristics of the ceramics, influencing, for example, their transport properties [9,10].

Traditionally, structure of ceramics is probed with scanning electron microscopy (SEM), porosimetry methods and etc. with complementary theoretical analysis [7,8,11–20]. However, the real structure of ceramics should be studied not only at atomic level, but also at void level. In this case the positron annihilation lifetime (PAL) spectroscopy can be used as method which is especially sensitive to free volumes in solids [21–24].

It was shown previously, that for spinel ceramics PAL data are decided by crystallographic features of individual grains, while structural disturbances due to grain contacts inside ceramics were a subject for additional complications [24–29]. This is why the measured positron annihilation lifetime spectra for functional ceramics can be adequately explained within combined model involving positron trapping and ortho-positronium (o-Ps) decaying (calculated within three-component procedure) [25,27–29]. In respect to this model the component with lifetime τ_1 reflects microstructural specifies of the mail spinel ceramics. The positron trapping component with lifetime τ_2 is attributed to free volumes near grain boundaries. The longest component with lifetime τ_3 is responsible to o-Ps annihilation [28,30] in nanopores of ceramics.

Thus, the main aim of this work is void and porous study of functional oxide materials taking the example of technologically micro and macro modified $Cu_{0.4}Co_{0.4}Ni_{0.4}Mn_{1.8}O_4$ ceramics using PAL technique in comparison with SEM and Hg-porosimetry methods.

2. Experimental

Functional $Cu_{0.4}Co_{0.4}Ni_{0.4}Mn_{1.8}O_4$ ceramics macro and micro modifications was prepared via traditional ceramic technology as was described in greater details elsewhere [24,31–38]. Equal molar amounts of initial powders were mixed in a planetary ball mill for 96 h in an environment with acetone to obtain mixture. The aqueous solution of polyvinyl alcohol was used for obtaining of the molding powder. Bilateral compression was performed in steel molds. After pressing these samples were sintered in a furnace at maximal temperature (T_s) 1100 °C for 2 h. According to our previous x-ray diffraction investigations, the micro and macro modified $Cu_{0.4}Co_{0.4}Ni_{0.4}Mn_{1.8}O_4$ ceramics are preferentially of single spinel phase with lattice parameter of a = 8.365 Å [24,39].

To validate PAL investigations performed, we divided the $Cu_{0.4}Co_{0.4}Ni_{0.4}Mn_{1.8}O_4$ ceramics into two groups presumably not affecting lifetime spectra — the $Cu_{0.4}Co_{0.4}Ni_{0.4}Mn_{1.8}O_4$-micro and $Cu_{0.4}Co_{0.4}Ni_{0.4}Mn_{1.8}O_4$-macro modified ceramics prepared by preliminary sifting of powder through fine (with 0.1 mm pores) and more rough sieve (0.5 mm pores). In both cases, the sizes of intrinsic pores are too large to change significantly positron annihilation spectra [31].

Structures of grains, grain boundaries and pores were studied using scanning electron microscopy (LEO 982 microscope) [26,28,31]. Pore size distribution in $Cu_{0.4}Co_{0.4}Ni_{0.4}Mn_{1.8}O_4$-micro and $Cu_{0.4}Co_{0.4}Ni_{0.4}Mn_{1.8}O_4$-macro modified ceramics in the region from 2 to 300 nm was investigated with Hg-porosimetry (POROSIMETR 4000) [28,40].

PAL measurements for $Cu_{0.4}Co_{0.4}Ni_{0.4}Mn_{1.8}O_4$ ceramics were performed using ORTEC spectrometer at temperature of 20 °C and relative humidity of ~35 % [26,29,41,42]. The isotope ^{22}Na was used as positron source. The two identical samples of ceramics were placed in the both sides of the source. The PAL spectra were treated by LT computer program [43]. For each pair of ceramic samples we used three measured positron annihilation spectra. The best results were obtained at three-component fitting procedure with parameters of each components (τ_1, I_1), (τ_2, I_2) and (τ_3, I_3). Such parameters as average positron lifetimes τ_{av}, positron lifetime in defect-free bulk τ_b and positron trapping rate in defects κ_d) were calculated using two-state positron trapping model [20,21,25–32]. The error-bars are ±0.03 ns for lifetimes, ±0.01 arb. units for intensities and ±0.01 ns^{-1} for positron trapping rate of defects [41,44].

3. Results and discussion

In respect to SEM investigations, the $Cu_{0.4}Co_{0.4}Ni_{0.4}Mn_{1.8}O_4$ ceramics contained large grains (~10 mm) as well as relatively sharp grain boundaries. So-called "closed" pores have a spherical form and are located mainly near grain boundaries. As it is obvious from electron micrographs (Fig. 1), $Cu_{0.4}Co_{0.4}Ni_{0.4}Mn_{1.8}O_4$-micro and $Cu_{0.4}Co_{0.4}Ni_{0.4}Mn_{1.8}O_4$-macro modified ceramics differ only by pores. The neatly shaping grains with comparatively tiny

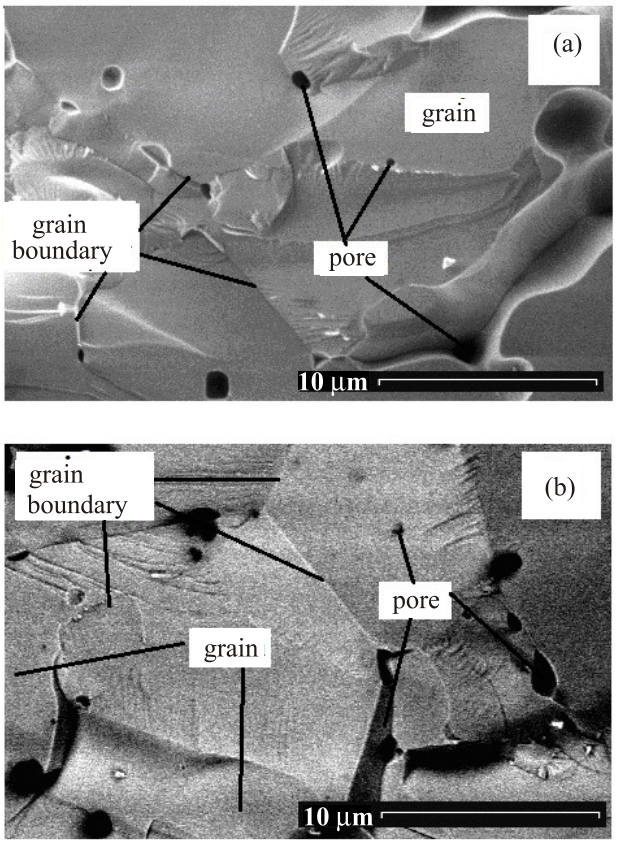

Fig. 1. Scanning electron micrographs of fracture section of $Cu_{0.4}Co_{0.4}Ni_{0.4}Mn_{1.8}O_4$-macro (a) and $Cu_{0.4}Co_{0.4}Ni_{0.4}Mn_{1.8}O_4$-micro (b) modified ceramics.

pores (~1 mm) are characteristic for $Cu_{0.4}Co_{0.4}Ni_{0.4}Mn_{1.8}O_4$-micro samples, while $Cu_{0.4}Co_{0.4}Ni_{0.4}Mn_{1.8}O_4$-macro ceramics contain similar crystalline grains with larger pores (reaching in size up to ~10 mm) [24].

Open pore size distributions of $Cu_{0.4}Co_{0.4}Ni_{0.4}Mn_{1.8}O_4$-micro and $Cu_{0.4}Co_{0.4}Ni_{0.4}Mn_{1.8}O_4$-macro modified ceramics are shown in Fig. 2. Such distributions cover significant amount of charge-transferring nanopores depending on sintering procedure and small amount of communication mesopores [40]. In contrast to humidity-sensitive $MgAl_2O_4$ ceramics, temperature-sensitive $Cu_{0.4}Co_{0.4}Ni_{0.4}Mn_{1.8}O_4$ ceramics practically do not possess outside-delivering macropores depending on specific surface area of initial powder [28]. Thus, $Cu_{0.4}Co_{0.4}Ni_{0.4}Mn_{1.8}O_4$ ceramics prepared at 1100 °C exhibit so-called one-modal pore size distribution with maximum position near 2 nm and double-maximum near 2.3 and 5.5 nm for $Cu_{0.4}Co_{0.4}Ni_{0.4}Mn_{1.8}O_4$-macro and $Cu_{0.4}Co_{0.4}Ni_{0.4}Mn_{1.8}O_4$-micro modified ceramics, respectively (Fig. 2).

Typical PAL spectrum for $Cu_{0.4}Co_{0.4}Ni_{0.4}Mn_{1.8}O_4$ ceramics deconvoluted into three components are shown in Fig. 3. This spectrum is characterized by peak and region of fluent decaying of counts in time. The mathematical decomposition of such curve can be described as a sum of decreasing exponents with different power-like indexes reciprocal to positron lifetimes [45].

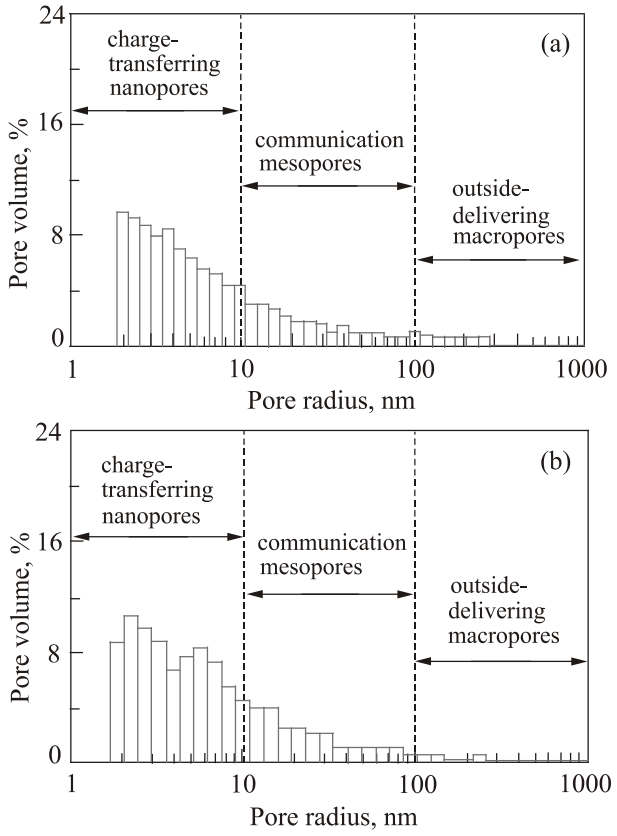

Fig. 2. Pore size distributions of $Cu_{0.4}Co_{0.4}Ni_{0.4}Mn_{1.8}O_4$-macro (a) and $Cu_{0.4}Co_{0.4}Ni_{0.4}Mn_{1.8}O_4$-micro (b) modified ceramics.

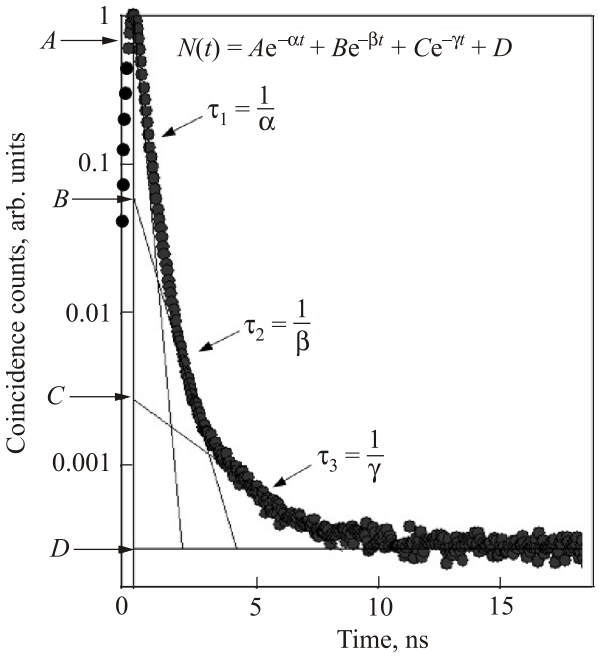

Fig. 3. Typical peak-normalized positron lifetime spectra for studied $Cu_{0.4}Co_{0.4}Ni_{0.4}Mn_{1.8}O_4$ spinel ceramics.

Let's try to discuss the results (Table 1) obtained within positron trapping model by accepting that structural peculiarities of spinel ceramics is associated mainly in the first PAL component (τ_1, I_1). The second component (τ_2, I_2) corresponds directly to free-volume positron traps (voids in the form of vacancy-like clusters, agglomerates, etc.) located near grain boundaries [21,24]. It means that input of the first component in the PAL spectra will be, in part, a determinant of the average electron density distribution reflected structural compactness of the testes network. The τ_2 lifetime is associated with the size of voids and the intensity I_2 is proportional to the amount of voids in the case of the same defect-free bulk annihilation lifetime [25,29]. The third component (τ_3, I_3) corresponds to o-Ps annihilation in nanopores. In spite of small value of I_3 intensity (2%), this component cannot be removed without losses in the quality of the fitting procedure. The similar component was detected in many porous materials with different structural type [26,27]. In addition, the third component can de related with o-Ps "pick-off" annihilation in water absorbed by materials [27,28]. We don't exclude the meaning of other positron annihilation channels in this PAL component too, such as para-positroniun (p-Ps) decaying with character lifetime of 0.125 ns [21]. But their influence is negligibly small, if the above requirement on close positron affinity will be more or less kept within a whole positron-trapping medium [46].

As it was shown in Table 1 and Table 2, micro and macro structuration of $Cu_{0.4}Co_{0.4}Ni_{0.4}Mn_{1.8}O_4$ ceramics during preparation does not influence their fitting parameters. As a result, such positron trapping modes as positron lifetime in defect-free bulk τ_b, average positron lifetime τ_{av}, positron

Table 1. Fitting parameters of LT computer program describing positron annihilation in the studied ceramics

Sample	Fitting parameters						Component input		
	τ_1, ns	I_1, arb. units	τ_2, ns	I_2, arb. units	τ_3, ns	I_3, arb. units	$\tau_1 I_1$, ns	$\tau_2 I_2$, ns	$\tau_3 I_3$, ns
$Cu_{0.4}Co_{0.4}Ni_{0.4}Mn_{1.8}0_4$-macro	0.21	0.78	0.37	0.20	1.85	0.02	0.16	0.07	0.04
$Cu_{0.4}Co_{0.4}Ni_{0.4}Mn_{1.8}0_4$-micro	0.22	0.77	0.38	0.21	1.83	0.02	0.17	0.08	0.04

trapping rate of defect κ_d, size of extended defects, where positrons are trapped ($\tau_2 - \tau_b$), and ratio represents the nature of these defects (τ_2/τ_b) [21,42] remain unchanged. Obviously, pores of large examination by SEM and Hg-porosimetry do not modify significantly the measured positron lifetime spectra, testifying in a favor of correctness of the performed measuring and fitting procedures.

As was shown early in [24], the potential positron traps in functional spinel-type ceramics are tetrahedral and octahedral cation vacancies. The average volume of these tetrahedrons V_{tetra} and octants V_{octa} can be selected as free-volume parameters for spinel-structured ceramics.

The radii of tetrahedral and octahedral sites in a spinel structure can be calculated using lattice parameter a [24]:

$$R_{\text{tetra}} = \sqrt{3}\left(u - \frac{1}{4}\right)a - R_0, \quad (1)$$

$$R_{\text{octa}} = \left(\frac{5}{8} - u\right)a - R_0, \quad (2)$$

where u is oxygen parameter and R_0 is oxygen atom with radius of 1.32 Å.

The oxygen parameter u in oxide spinels is near 0.385 and insignificantly depends on cation type [26,39]. The radius of tetrahedral vacancies in $Cu_{0.4}Co_{0.4}Ni_{0.4}Mn_{1.8}O_4$ ceramics is 0.64 Å, which gives V_{tetra} in spherical approximation ~1.10 Å^3. The volume of octahedral vacancies V_{octa} is ~1.37 Å^3. As it was noted [24], positrons have a preference to annihilate in octahedral vacancy sites as it follows from charge density distribution in partially inverted spinel structures. But the calculated ratio between the first component inputs in the PAL spectra for previously studied $MgAl_2O_4$ ceramics [24,29] and $Cu_{0.4}Co_{0.4}Ni_{0.4}Mn_{1.8}O_4$ ceramics (0.78) is closer to the ratio between corresponding volumes of tetrahedral vacancies (0.76) rather than octahedral ones (0.69). Consequently, in the studied $Cu_{0.4}Co_{0.4}Ni_{0.4}Mn_{1.8}O_4$ ceramics in contrast to nanocrystalline ferrites [21], positron trapping in tetrahedral vacancies predominates in the first PAL component. The positron trapping in octahedral vacancies is character to inverse spinel structure.

It is evident that octahedral monovacancies themselves do not play a decisive role in the second component of PAL spectra. This component is associated with more extended agglomerates such as vacancy-like clusters and nanovoids. They appear, as a rule, near grain boundaries, where ceramics structure is more defective. The characteristic volumes of these clusters are larger in ceramics with a more stretched pore structure. In seats where ceramics are composed with very small grains with divaricated grain boundaries and tiny pores, the positrons are prepped more effective.

Recently, PAL spectroscopy started to be used as an alternative porosimetry technique to characterize the local free volumes first of all in both open and closed nanopores [21,30,47–49]. The PAL method is particularly effective when Ps is formed. In disordered solids Ps is usually organized in two ground state (p-Ps and o-Ps) and localized in the pores and free-volume [47–49]. Usually, quantification is based on the analysis of o-Ps lifetime (the lifetimes of the third component τ_3 in $Cu_{0.4}Co_{0.4}Ni_{0.4}Mn_{1.8}O_4$ ceramics corresponds to o-Ps lifetime). The o-Ps "pick-off" annihilation depends on the size of holes and gives additional important information on the void structure of the materials [49]. Despite small I_3 intensity for $Cu_{0.4}Co_{0.4}Ni_{0.4}Mn_{1.8}O_4$ ceramics, it is possible to estimate the average nanopores size from o-Ps lifetime in a given material [51]. Assuming approximately spherical shape of the free volume, the o-Ps lifetime ($\tau_{o\text{–}Ps}$) in oxide materials can be related to the average radius of pores (R) by semiempirical Tao–Eldrup equation [51,52].

$$\tau_{\text{o-Ps}} = \left[2\left(1 - \frac{R}{R+\Delta R} + \frac{1}{2\pi}\sin\left(\frac{2\pi R}{R+\Delta R}\right)\right) + 0.007\right]^{-1}, \quad (3)$$

where ΔR is the empirically determined parameter (in the classical case $\Delta R \approx 0.1656$ nm), describing effective thickness of the electron layer responsible for the "pick-off" annihilation of o-Ps in the pore [51,52].

In functional $Cu_{0.4}Co_{0.4}Ni_{0.4}Mn_{1.8}O_4$ ceramics there is one o-Ps PAL component with small intensity (2%). Therefore, τ_3 lifetime can be related to corresponding pores via Tao–Eldrup model. The $\tau_{o\text{-}Ps}$ value of around ~1.8 ns (τ_3 in Table 1) corresponds to nanopores with radius (R) distribution centered near ~0.27 nm. This result are addition to Hg-porosimetry measurements. In addition, it should be noted, that porosimetry methods are limited to open pores, which should have an access to the environment to be determined. On the other hand, PAL spectroscopy can probe both open and closed pores in functional oxide ceramics of sizes ranging from atomic scale to several tens of nanometers [28,50].

5. Conclusions

In conclusion, the usefulness of PAL technique combined with Hg-porosimetry and SEM methods to study of void-porous structure of functional $Cu_{0.4}Co_{0.4}Ni_{0.4}Mn_{1.8}O_4$ ceramics micro and macro modifications is demonstrated. The adequate characterization methodology for free-volume defects in the sintered spinels can be developed in terms of positron trapping model with small mixing from ortho-positronium decaying chanell.

The first component on the lifetime spectra shown microstructure specificity of the spinel ceramics with octahedral and tetrahedral cation vacancies. The extended defects near grain boundaries (voids) are reflected by the second component at the level of ~ 0.4 ns. The small third component is due to "pick-off" annihilation of o-Ps in the intergranual nanopores. The observed o-Ps lifetime ~1.8 ns is related to the nanopores with radius of ~2.7 nm based on classic Tao–Eldrup equation. The reported data gives additional information to Hg-porosimetry and SEM results.

Acknowledgements: H. Klym would like to thank the support via the Project DB/KIBER (No. 0115U000446) and A.I. Popov thanks Latvian State research program IMIS2 for a funding.

1. A. Rousset, R. Legros, and A. Lagrange, *J. Europ. Ceram. Soc*. **13**, 185 (1994).
2. G. Elssner, H. Hover, G. Kiessler, and P.Wellner, *Ceramics and Ceramic Composites: Materialographic Preparation*, Amsterdam-Lausanne-New York-Shannon-Singapore-Tokyo Elsevier (1999).
3. D. Houivet, J. Bernard, and J.M. Haussonne, *J. Europ. Ceram. Soc.* **24**, 1237 (2004).
4. N. Setter, *J. Europ. Ceram. Soc*. **21**, 1279 (2001).
5. P. Umadevi and C.L. Nagendra, *Sensors and Actuators B* **96**, 114 (2002).
6. S. Fritsch, J. Sarrias, M. Brieu, J.J. Couderc, J.L. Baudour, E. Snoeck, and A. Rousset, *Solid State Ionics* **109**, 229 (1998).
7. G. de With and H.J. Glass, *J. Europ. Ceramic Soc*. **17**, 753 (1997).
8. P. Davies and V. Randle, *Mater. Science Technol*. **17**, 615 (2001). DOI:10.1179/026708301101510384
9. D. Gryaznov, J. Fleig, and J. Maier, *Solid State Ionics* **177**, 1583 (2006).
10. D. Gryaznov, J. Fleig, and J. Maier, *Solid State Sciences* **10**, 754 (2008).
11. F. Tang, H. Fudouzi, T. Uchikoshi, and Y. Sakka, *J. Europ. Ceramic Soc*. **24**, 341 (2004).
12. S. Bellucci, I. Bolesta, I. Karbovnyk, R. Hrytskiv, G. Fafilek, and A.I. Popov, *J. Phys.: Condens. Matter* **20**, 474211 (2008). DOI:10.1088/0953-8984/20/47/474211
13. S. Bellucci, A.I. Popov, C. Balasubramanian, G. Cinque, A. Marcelli, I. Karbovnyk, V. Savchyn, and N. Krutyak, *Radiat. Measur*. **42**, 708 (2007).
14. A. Šutka, M. Millers, N. Döbelin, R. Pärna, M. Vanags, M. Maiorov, J. Kleperis, T. Käämbre, U. Joost, E. Nõmmiste, V. Kisand, and M. Knite, *Phys. Status Solidi A* **212**, 796 (2015).
15. A. Voloshynovskii, P. Savchyn, I. Karbovnyk, S. Myagkota, M. Cestelli Guidi, M. Piccinini, and A.I. Popov, *Solid State Commun*. **149**, 593 (2009).
16. F. Wang, W.W. Huang, S.Y. Li, A. Q Lian, X.T. Zhang, and W. Cao, *J. Magn. Magn. Mater*. **340**, 5 (2013).
17. I. Karbovnyk, S. Piskunov, I. Bolesta, S. Bellucci, M. Cestelli Guidi, M. Piccinini, E. Spohr, and A.I. Popov, *Europ. Phys. J. B* **70**, 443 (2009).
18. P. Savchyn, I. Karbovnyk, V. Vistovskyy, A. Voloshinovskii, V. Pankratov, M. Cestelli Guidi, C. Mirri, O. Myahkota, A. Riabtseva, N. Mitina, A. Zaichenko, and A.I. Popov, *J. Appl. Phys*. **112**, 124309 (2012).
19. A. Gatelyte, J. Senvaitiene, D. Jasaitis, A. Beganskiene, and A. Kareiva, *Chemija* **22**, 19 (2011).
20. R. I. Eglitis and G. Borstel, *Phys. Status Solidi A* **202**, R13

Table 2. Positron trapping modes in the studied ceramics calculated within two-state positron trapping model and free-volume characteristics

Sample	Free-volume characteristics			Positron trapping modes				
	R_{octa}, Å	R_{tetra}, Å	R_{pore}(Tao–Eldrup), nm	τ_{av}, ns	τ_b, ns	κ_d, ns^{-1}	$\tau_2 - \tau_b$, ns	τ_2/τ_b
$Cu_{0.4}Co_{0.4}Ni_{0.4}Mn_{1.8}0_4$-macro	0.69	0.64	0.274	0.24	0.23	0.4	0.14	1.6
$Cu_{0.4}Co_{0.4}Ni_{0.4}Mn_{1.8}0_4$-micro			0.272	0.25	0.24	0.4	0.14	1.6

(2005).
21. R. Krause-Rehberg and H.S. Leipner, *Positron Annihilation in Semiconductors. Defect Studies*, Springer-Verlag, Berlin-Heidelberg-New York (1999).
22. Abu Zayed Mohammad Saliqur Rahman, Zhuoxin Li, Xingzhong Cao, Baoyi Wang, Long Wei, Qiu Xu, and Kozo Atobe, *Nuclear Instrum. Meth. Phys. Res. B* **335**, 70 (2014). DOI:10.1016/j.nimb.2014.06.002
23. Takuji Suzuki, Hiroki Terabe, Shimpei Iida, Takashi Yamashita, and Yasuyuki Nagashima, *Nuclear Instrum. Meth. Phys. Res. B* **334**, 40 (2014).
24. V. Balitska, J. Filipecki, A. Ingram, and O. Shpotyuk, *Phys. Status Solidi C* **4**, 1317 (2007).
25. H. Klym and A. Ingram, *J. Phys.: Confer. Ser*. **79**, 012014 (2007).
26. H. Klym, A. Ingram, O. Shpotyuk, J. Filipecki, and I. Hadzaman, *J. Phys.: Confer. Ser*. **28**9, 012010 (2011).
27. J. Filipecki, A. Ingram, H. Klym, O. Shpotyuk, and M. Vakiv, *J. Phys.: Confer. Ser*. **79**, 012015 (2007).
28. H. Klym, A. Ingram, I. Hadzaman, and O. Shpotyuk, *Ceram. Intern.* **40**, 8561 (2014).
29. H. Klym, A. Ingram, O. Shpotyuk, J. Filipecki, and I. Hadzaman, *IOP Confer. Ser.: Mater. Science Engin*. **15**, 012044 (2010).
30. Y.C. Jean, P.E. Mallon, and D.M. Schrader, *Principles Application of Positron and Positronium Chemistry*, Word Scientific, Singapore (2003).
31. O. Shpotyuk, V. Balitska, I. Hadzaman, and H. Klym, *J. Alloys Compounds* **509**, 447 (2011).
32. I. Hadzaman, H. Klym, O. Shpotuyk, and M. Brunner, *Acta Phys. Polonica A* **117**, 234 (2010).
33. H. Klym, I. Hadzaman, O. Shpotyuk, Q. Fu, W. Luo, and J. Deng, *Solid State Phenom*. **200**, 156 (2013).
34. M. Vakiv, I. Hadzaman, H. Klym, O. Shpotyuk, and M. Brunner, *J. Phys.: Confer. Ser*. **289**, 012011 (2011).
35. H. Klym, I. Hadzaman, O. Shpotyuk, and M. Brunner, *Nanoscale Res. Lett.* **9**, 149 (2014).
36. I. Hadzaman, H. Klym, and O. Shpotyuk, *Intern. J. Nanotechnol.* **11**, 843 (2014).
37. H. Klym, I. Hadzaman, A. Ingram, and O. Shpotyuk, *Canadian J. Phys.* **92**, 822 (2014).
38. H. Klym, V. Balitska, O. Shpotyuk, and I. Hadzaman, *Microelectron. Reliab*. **54**, 2843 (2014).
39. O. Shpotyuk, V. Balitska, M. Brunner, I. Hadzaman, and H. Klym, *Physica B* **459**, 116 (2015).
40. A. Bondarchuk, O. Shpotyuk, A. Glot, and H. Klym, *Revista Mexicana de Fisica* **58**, 313 (2012).
41. O. Shpotyuk, A. Ingram, M. Shpotyuk, and J. Filipecki, *Nuclear Instrum. Meth. Phys. Res. B* **33**8, 66 (2014).
42. I. Karbovnyk, I. Bolesta, I. Rovetskii, S. Velgosh, and H. Klym, *Mater. Science-Poland* **32**, 391 (2014).
43. J. Kansy, *Nucl. Instrum. Meth. Phys. Res. A* **374**, 235 (1996).
44. O. Shpotyuk, L. Calvez, E. Petracovschi, H. Klym, A. Ingram, and P. Demchenko, *J. Alloys Comp.* **582**, 232 (2014).
45. D.M. Bigg, *Polym. Engin. Science* **36**, 737 (1996).
46. H.E. Hassan, T. Sharshar, M.M. Hessien, and O.M. Hemeda, *Nuclear Instrum. Meth. Phys. Res. B* **304**, 72 (2013).
47. O.E. Mogensen, *Positron Annihilation in Chemistry*, Springer, Berlin (1995).
48. H. Nakanishi, Y.C. Jean, D.M. Schrader, and Y.C. Jean, in: *Positron and Positronium Chemistry*, Elsevier, Amsterdam (1998).
49. G. Dlubek, A. Sen Gupta, J. Pionteck, R. Hassler, R. Krause-Rehberg, H. Kaspar, and K.H. Lochhaas, *Macromolecules* **38**, 429 (2005).
50. R. Golovchak, Sh. Wang, H. Jain, and A. Ingram, *J. Mater. Res*. **27**, 2561 (2012).
51. S.J. Tao, *J. Chem. Phys*. **56**, 5499 (1972).
52. M. Eldrup, D. Lightbody, and J.N. Sherwood, *Chem. Phys*. **63**, 51 (1981).